Plastic Strain Hardening Effect on Ductile Fracture Resistance

P. A. Eikrem[1], Z. L. Zhang[1], E. Østby[2] and B. Nyhus[2]
[1]*Norwegian University of Science and Technology, Trondheim, Norway;*
[2]*SINTEF Materials and Chemistry, Trondheim, Norway*

Abstract: The effect of strain hardening on ductile fracture resistance is unclear and contradictory in the literature. The effect is also difficult to verify experimentally. In this paper the complete Gurson model developed by the authors has been applied to numerically investigate the effect of strain hardening on ductile fracture resistance. It has been found that the predicted fracture resistance pattern depends on the element damage strain and void coalescence criterion. When an unrealistically large critical void volume fraction is used the plastic strain hardening displays a positive effect on the predicted crack resistance. However, when Thomason's plastic limit load based void coalescence criterion is used (the so-called complete Gurson model) plastic strain hardening has shown to reduce the crack resistance.

1. Introduction

The ductile crack growth plays an important role in the analysis of the fracture behavior of structures. It is known that ductile crack growth in metals is a result of nucleation, growth and coalescence of micro voids. The best known model to describe ductile fracture is the Gurson model [1-3]. Several numerical studies have been carried out to investigate the effect of the input parameters of the Gurson model on material's ductile resistance curve [4-6]. Among the parameters studied is the strain hardening exponent. The effect of plastic strain hardening reported by Østby et al. [5] and Eikrem et al. [6] is not in correspondence with the results by Xia and Shih [4]. The present study aims to explore this contradiction by using different versions of the Gurson models.

2. Numerical procedures and materials

A single edge notched tension (SENT) specimen is applied to study the ductile fracture behavior. Figure 1 shows the SENT specimen geometry and the finite element mesh used. The initial crack size (a) considered is 4 mm and other dimensions are a/w=0.143 and L/w=4.1. A remote displacement controlled boundary condition (clamped) was applied. Because of the symmetry, half of the SENT specimen has been modeled with 4-node plane strain elements in ABAQUS. Close to the crack tip a region with uniform mesh size (4.8 mm ahead of the initial crack tip and 0.7 mm above the symmetrical line) is used to simulate the ductile crack growth. The uniform element size in this local region is 0.1x0.1 mm. A user material subroutine UMAT has been applied to implement the

Gurson model using the numerical algorithms developed by Zhang [7]. Large deformation effect is considered.

In order to study the effect of plastic strain hardening, a model material with the following power law hardening rule has been utilized:

$$\sigma_f = \sigma_0 \left(1 + \frac{\varepsilon^p}{\varepsilon_0} \right)^n \tag{1}$$

where σ_f is the flow stress, σ_0 is the yield stress, ε^p is the equivalent plastic strain , ε_0 is the yield strain and *n* is the hardening exponent. In all the analyses σ_0=400MPa and the Young's modulus *E* = 200GPa and Poisson ratio ν = 0.3 are fixed. Three hardening exponents *n*=0.05, 0.10 and 0.20 have been studied.

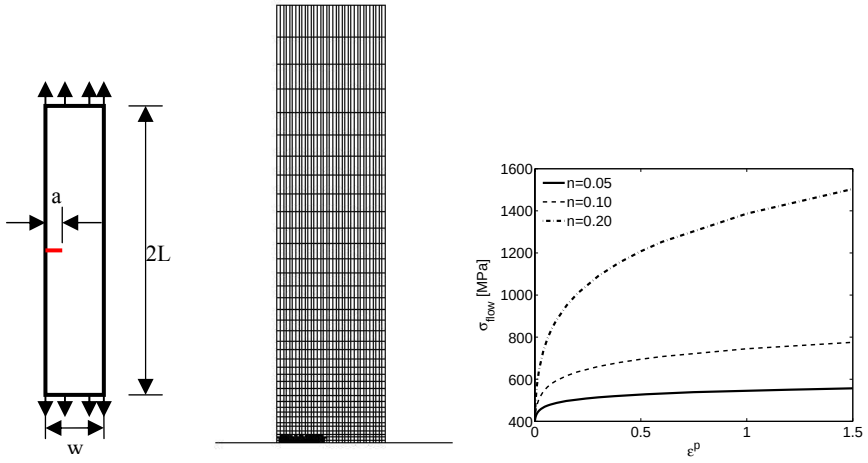

Figure 1 Schematic plot of the SENT specimen, the finite element mesh and the materials used.

The Gurson model used has the following form:

$$\phi\left(q, \sigma_f, f, \sigma_m\right) = \frac{q^2}{{\sigma_f}^2} + 2q_1 f \cosh\left(\frac{3q_2\sigma_m}{2\sigma_f}\right) - 1 - \left(q_1 f\right)^2 = 0$$

where *q* is the von Mises stress, f is the void volume fraction and σ_m is the mean normal stress component. q_1 and q_2 are the parameters introduced by Tvergaard [2,3] to modify the original Gurson model. In the original Gurson model $q_1 = q_2 =$ 1.0. An initial void volume fraction f_0=0.005 is used in all analyses.

Several people have used the Gurson model based computational approach to study the effect of strain hardening on ductile fracture resistance. Xia and Shih [4]

reported that raising materials' hardening capacity, and keeping other parameters fixed, increases the *J* resistance curve. Similar study has also been carried out recently by Østby et al. [5] and Eikrem et al. [6], using the complete Gurson model developed by the authors [8]. The results by [5, 6] are not in accordance with the ones by Xia and Shih [4]. In these numerical studies the treatment of void coalescence in the Gurson model and the corresponding coalescence parameters used are different. A so-called critical void volume fraction equal to 0.2 has been used by Xia and Shih [4], before the element loading capacity is gradually reduced to zero in 20 steps. In [5,6] the critical void volume fraction was determined by Thomason's plastic limit load model (the complete Gurson model [8]), the critical void volume fraction automatically determined is between 0.02-0.04. In addition, the q_1=1.25 has been used by Xia and Shih [4] while Østby et al. [5] and Eikrem et al. [6] used q_1=1.50. In the following, the effect of void coalescence criterion and parameters on the predicted ductile crack resistance will be explored.

3. Results and discussion

3.1 Resistance curves predicted by the complete Gurson model

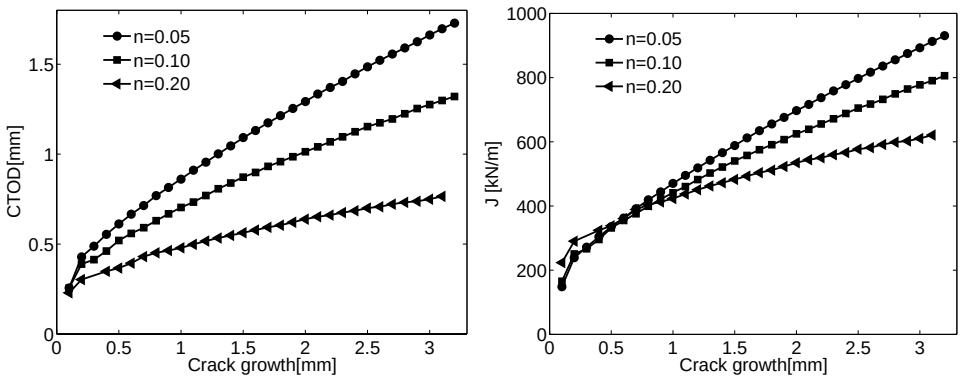

Figure 2 Resistance curves for *n*=0.05, 0.10 and 0.20. σ_0=400MPa, *E*=200GPa, ν=0.3 and f_0=0.005. q_1=1.5 and q_2=1.0. The complete Gurson model is used. a) CTOD resistance curve and b) J resistance curve.

The effect of plastic strain hardening on fracture resistance reported by Eikrem et al. [6] is re-produced in Figure 2a. The results were obtained by using the complete Gurson model with q_1=1.5 and q_2=1.0**.** The fracture resistance behavior has been measured in terms of both the crack tip opening displacement (CTOD) and the *J* integral. A clear trend for the CTOD resistance curve can be observed. The plastic strain hardening exponent has negligible effect on the crack initiation CTOD, and a strong hardening will decrease the CTOD resistance. A more complex behavior is observed in Figure 2b for the *J* resistance curve. Crack initiation occurs at a slightly higher *J* for strong hardening. However, the tangent of the *J* resistance curve decreases with the increase of strain hardening. This

causes the resistance curves to cross each other at a crack growth about 0.6 mm. For larger crack growth, the *J* resistance behavior is similar to that of the CTOD resistance curve – increasing hardening reduces the fracture resistance. The *J* resistances in Fig 2 are in correspondence to the results of Østby [5].

3.2 Resistance curve predicted by the complete Gurson model f_c=0.2

The so-called critical void volume fraction has been widely used in the literature to describe void coalescence. The value of the critical void volume fraction is often selected arbitrary. The resistance curves predicted by using the critical void volume fraction 0.2 suggested by Xia and Shih [4] are presented in Fig. 3 for the case with q_1=1.5 and in Fig. 4 for q_1=1.25, respectively. It is interesting to note that the CTOD resistances predicted by the Gurson model using the critical void volume fraction 0.2 with both q_1=1.5 and 1.25 display the same trend as the CTOD resistance curve predicted using the complete Gurson model, see Fig. 2.

Both Figs. 3 and 4 show that the plastic strain hardening will positively influence the *J* resistance curves. Decreasing q_1 from 1.50 to 1.25 increases the *J* at crack initiation. For the case with large q_1 which implies an accelerated void growth and loss of load carrying capacity, the *J* resistance curves of different strain hardening exponents seem to converge and eventually cross each other in a later stage. The crack growth in the analyses is limited by the mesh design and longer crack growth was not possible.

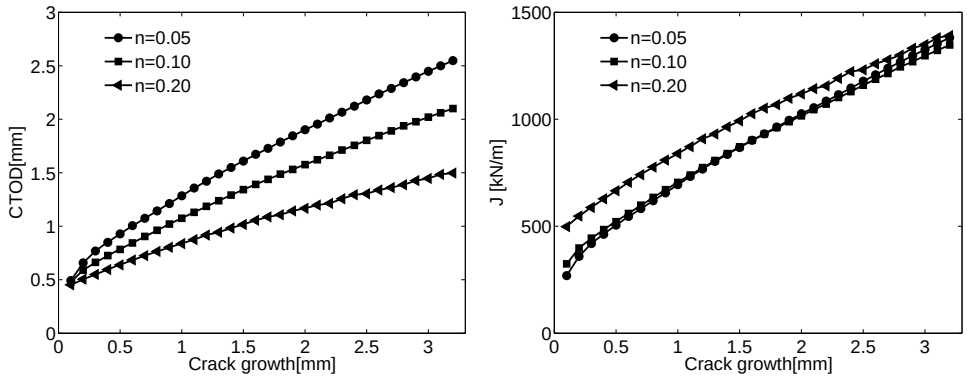

Figure 3 Resistance curves for *n*=0.05, 0.10 and 0.20. σ_0=400MPa, E=200GPa, ν=0.3, f_0=0.005 and f_c=0.2. q_1=1.5 and q_2=1.0. a) CTOD resistance curve and b) *J* resistance curve.

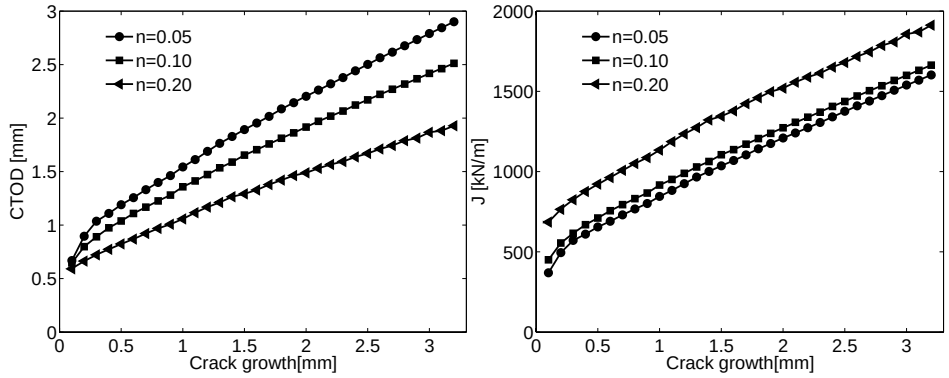

a) **b)**

Figure 4 Resistance curves for n=0.05, 0.10 and 0.20. σ_0=400MPa, E=200GPa, v=0.3, f_0=0.005 and f_c=0.2. q_1=1.25 and q_2=1.0. a) CTOD resistance curve and b) J resistance curve.

When a smaller q_1=1.25 is used, Fig. 4, the predicted *J* resistance curves for different strain hardening exponents become parallel to each other. A distinct trend is observed - increasing the strain hardening increases the *J* resistance curve. The predicted *J* resistance behaviour thus becomes opposite to the CTOD resistance curve.

3.3 Discussions

Fig. 5 shows the equivalent plastic strain and stress triaxiality distribution ahead of the initial crack tip at crack initiation for the cases with the complete Gurson model. At crack initiation there is a minor difference between stress triaxiality and equivalent plastic strain. At further crack growth stress triaxiality increases significantly with the increase of strain hardening. Equivalent plastic strain has the opposite trend, the equivalent plastic strain decreases with the increase of hardening.

This observation explains why CTOD at crack initiation is approximately the same for different hardenings while the CTOD resistance is higher for weaker hardening materials at further crack growth, Fig. 2. The same explanation can also be applied to the CTOD resistance behavior in Figs. 3-4. CTOD is a measure of the plastic deformation at the crack tip.

The *J*-integral is a measure of the energy release rate at crack growth. The J-integral scales with the area under the force-displacement curve to the SENT specimen. The global deformation to the specimen is linked to the deformation needed to start crack growth. At crack initiation, the first element is damaged at approximately the same equivalent plastic strain for the three hardening exponents considered and there are no larger differences among the stress triaxialities for the three cases. To achieve the same equivalent plastic strain a higher stress is needed for the material with a stronger strain hardening exponent. This results in a higher initiation toughness for the stronger material.

The opposite trends of the *J* resistance at large crack growth are not easy to explain. It can probably be explained by the differences in the equivalent plastic strain levels in front of the crack tip caused by the different void coalescence criteria applied. The equivalent plastic strain distribution at crack initiation for the case with f_c=0.2. q_1=1.25 is shown in Fig. 6. Because of the large f_c and small q_1 the equivalent plastic strain at crack initiation is about two times that of the values in Fig. 5. When the complete Gurson model is used, the difference in flow stress is not sufficiently large to compensate the large difference in equivalent plastic strains and the *J* resistance of a weak hardening material could be higher than that of a stronger hardening material. When a large critical void volume fraction together with a small q_1 (f_c=0.2. q_1=1.25) is used, the equivalent plastic strain at crack growth is doubled, but the differeece in equivalent plastic strain is nearly the same, see Fig. 6. Because of a power strain hardening material law is used (Eq. (1)), this will induce significant increase in the flow stress for a strong hardening material (Fig. 1) and result in higher *J* resistance.

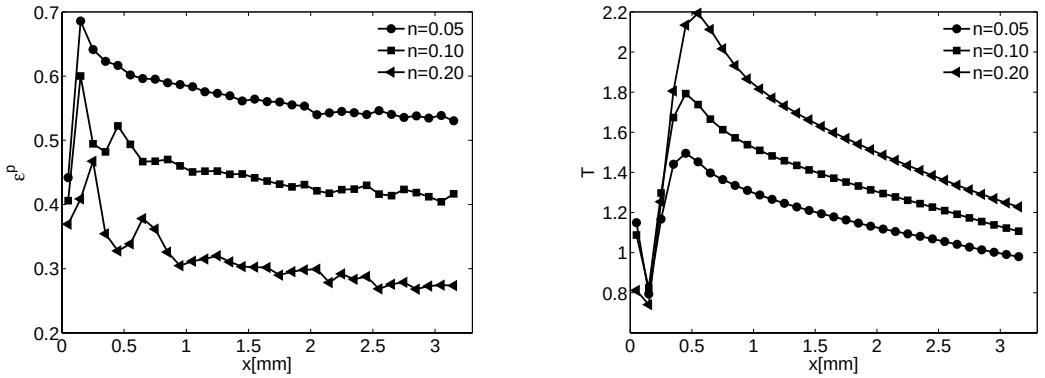

Figure 5 a) Equivalent plastic strain at element damage ahead of the original crack tip and b) stress triaxiality when one element is damaged. σ_0=400MPa, E=200GPa, v=0.3 and f_0=0.005. q_1=1.5 and q_2=1.0. Complete Gurson model was sused.

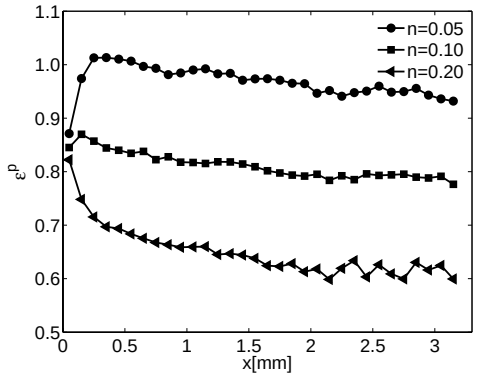

Figure 6 Equivalent plastic strain at element damage ahead of the original crack tip. σ_0=400MPa, *E*=200GPa, v=0.3 and f_0=0.005. q_1=1.5 and q_2=1.0. f_c=0.20.

4. Concluding remarks

It should be noted that it is very difficult to experimentally verify the plastic strain hardening effect on the fracture resistance, because it is nearly impossible to produce materials with different strain hardening capacities while keeping other parameters (yield stress, initial void volume fraction) unchanged.

The Gurson model with different void coalescence criterion and parameters have been applied to study the behavior of fracture resistance curves. The results show that the different behavior of *J* resistance curves reported in the literature is attributed to the different versions of the Gurson model used. All the results indicate that the crack initiation toughness in terms of *J* increases with the increase of strain hardening. However, when the complete Gurson model is applied, the failure strain at crack growth is relatively small and decreasing hardening seems to increase the fracture resistance. However, when a large critical void volume fraction (for example 0.2) is applied, the crack tip failure strain becomes very large and increasing plastic strain hardening will increase the *J* resistance curve. The exact reason for this observation remains to be further explored.

In this study the Tvergaard parameters q_1 and q_2 have been kept as constants independent of the strain hardening exponents. Further work will test strain hardening dependent Gurson model, for example, the one proposed by Gao [9].

5. References

1. Gurson A.L., Continuum theory of ductile rupture by void nucleationand growth: Part 1-yield criteria and flow rules for porous ductile media, *Journal of Engineering Materials and Technology*, **99** (1977) 2–15.

2. Tvergaard V., Influence of voids on shear band instabilities under plane strain conditions *Int. J. Fracture*, **17** (1981) 389–407.

3. Tvergaard V. and Needleman A., Analysis of the cup-cone fracture in a round tensile bar, *Acta Metall*, **32** (1984) 157–169.

4. Xia L. and Shih F., Ductile crack growth-i. a numerical study using computational cells with microstructurally-based length scales, *J. Mech. Phys. Solids*, **43** (1995) 223–259.

5. Østby E., Thaulow C. and Zhang Z.L., Numerical simulation of specimen size and mismatch effect in ductile crack growth – Part I: Tearing resistance and crack growth paths, *Engineering Fracture Mechanics,* **74** (2007) 1770-1792.

6. Eikrem P.A., Zhang Z.L., Østby E. and Nyhus B., Numerical study on the effect of prestrain history on crack resistance of SENT specimens, *Engineering Fracture Mechanics*, **75**(2008) 4568-4582

7. Zhang Z.L. and Niemi E., A class of generalized mid-point algorithms for Gurson-Tvergaard continuum damage material model, *International Journal for Numerical Methods in Engineering*, **38** (1995) 2033-2053.

8. Zhang Z.L., Thaulow C. and Ødegård J., A complete Gurson model approach for ductile fracture, *Engineering Fracture Mechanics*, **67** (2000) 155–168.

9. Gao X., Numerical modeling of crack growth in ductile-brittle transition regime, *Ph.D thesis*, Brown University, England, 1998.